Communication

Synthesis and Spectrophotometric Studies of Heterocyclic Bay-Substituted Naphthalenediimide Colorimetric pH Indicators

Filippa Magro, Luke Camenzuli and David C. Magri *

Department of Chemistry, Faculty of Science, University of Malta, MSD 2080 Msida, Malta; luke.camenzuli.16@um.edu.mt (L.C.)
* Correspondence: david.magri@um.edu.mt

Abstract: Four naphthalenediimide colorimetric pH indicators were synthesized with *N,N*-dimethylethyleneamine at the imide positions and with 5- to 7-membered heterocyclic rings at the bay positions, namely pyrrolidine, morpholine, piperidine and azepane. The pH indicators are constructed in a modular *receptor–spacer–fluorophore–spacer–receptor* format based on a photoinduced electron transfer (PET) design. The compounds were studied by UV–visible absorption and steady-state fluorescence spectroscopy in 1:1 (*v/v*) methanol/water. Brilliant colour changes are observed between pH 2 and 4 due to an internal charge transfer (ICT) mechanism. Fluorescence *turn-on* enhancements range from 10–37 fold; however, the maximum fluorescence quantum yield in the presence of acid is <0.004, which is below naked eye detection. Hence, from the viewpoint of a human observer, these chemosensors function as colorimetric YES logic gates, and fluorimetric PASS 0 logic gates.

Keywords: naphthalenediimide; acid–base pH indicators; colorimetric; absorbance spectroscopy; internal charge transfer

1. Introduction

Naphthalenediimides (NDIs) are remarkable dyes that are attracting considerable attention in the design of ingenious molecular devices due to their ease of synthesis and electron accepting properties [1–5]. They are excellent components for studying photoinduced electron transfer in models for photosynthetic mimicry [6] and solar energy conversion [7]. Most conveniently, NDIs can be synthesized in as little as two steps from commercially available reagents. Core-substituted NDIs have rapidly emerged as a more attractive class of molecule. The additional substituents on the chromophore allow for the tuning of the solubility, optical and redox properties [7]. The resulting compounds are highly colourful in solution, and have different photophysical and redox properties than their core unsubstituted counterparts [8,9].

Past developments in the field of colorimetric and fluorometric NDI indicators have tended to focus on studies in organic solvents [10,11]. There has been some development of NDI chemosensors in aqueous solution and at physiological conditions of pH 6–8 for biological imaging within cells [12–15]. Other studies have demonstrated chemosensors for binding metal ions, particularly with crown ethers at the bay positions [16–19]. A few examples of NDI-based logic gates are also known [20–22].

The purpose of this study was to investigate NDIs as colorimetric and fluorimetric pH indicators as a platform for the development of Pourbaix sensors [23,24], fluorescent logic gates for acidity (pH) and oxidisability (pE), [25,26] based on photoinduced electron transfer [27]. In a recent study, we synthesized a core unsubstituted NDI molecule with an *electron-donor–spacer–fluorophore–spacer–receptor* format, with ferrocene as the electron donor and dimethylamino as the proton receptor [28]. We observed that the compound did not

function as a H^+, Fe^{3+}-driven AND logic gate as observed with perylenediimide [29] and naphthalenediimide-based Pourbaix sensors [25], but rather as a two-input PASS 0 logic gate (Table 1). In the presence of high H^+ and high Fe^{3+} (as oxidant), the fluorescence output was not enhanced according to AND logic [27], but rather remained in an 'off' state independent of the absence or presence of H^+ and Fe^{3+} inputs.

Table 1. Logic truth tables for double-input PASS 0 and AND gates.

		PASS 0	AND
Input (H^+)	**Input (Fe^{3+})**	**Output (Light)**	**Output (Light)**
0	0	0	0
1	0	0	0
0	1	0	0
1	1	0	1

In order to obtain a better understanding of this shortcoming, our strategy for this study was to design and synthesize NDI-based pH indicators constructed in a modular format based on a *receptor–spacer–fluorophore–spacer–receptor* format. In the past, we have developed water-soluble colorimetric and fluorimetric chemosensors via the incorporation of two negatively charged sulfonate moieties [30–32]. In this study, we planned for a series of NDI molecules that would have two positively charged dimethylamino moieties in acidic media. Furthermore, we purposely designed core-substituted NDI derivatives with heterocyclic substituents at the bay positions [33,34] of the aromatic ring in order to introduce an internal charge transfer (ICT) mechanism that would extend the absorbance and emission to longer wavelengths. Moreover, we rationalized that substitution with heterocyclic donors would avert the formation of aggregates via π–π interactions.

In this study, four molecules **1**–**4** were synthesized from 2,6-dibromo-1,4,5,8-naphthalenetetracarboxylic acid dianhydride (Figure 1). A dimethylamino (*receptor*) with an ethylene spacer was attached to the two imide positions of the NDI. The dibrominated NDI core was further modified by incorporating the following heterocyclic amines: pyrrolidine **1**, morpholine **2**, piperidine **3** or azepane **4**. The addition of a cyclic amine was hypothesized to introduce an ICT character and extend the absorbance to longer wavelengths and to prevent the formation of aggregates. The photophysical characteristics of **1**–**4** were studied by UV–vis absorption and fluorescence spectroscopy in 1:1 (*v/v*) methanol/water.
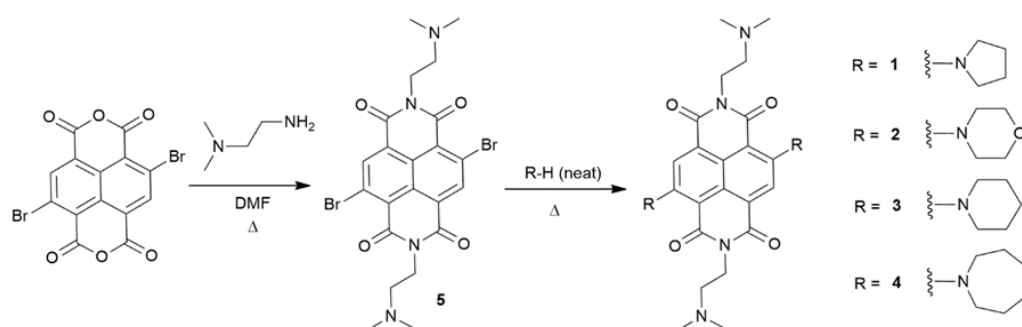

Figure 1. The synthesis of the naphthalenediimide (NDIs) indicators **1**–**4**.

2. Materials and Methods

2.1. Chemicals

2,6-Dibromonaphthalene-1,4,5,8-tetracarboxylic dianhydride (TCI Europe, Zwijndrecht, Belgium; >98.0%), pyrrolidine (TCI Europe, Zwijndrecht, Belgium, 98%), morpholine (Sigma Aldrich Chemie Gmbh, Steinheim, Germany, 99.0%), piperidine (Carlo Erba, Val de Reuil, France, 99%), azepane (Sigma Aldrich; 99%), N,N-dimethylethylenediamine (Sigma

Aldrich; >95.0%), anthracene (Alfa Aesar, Ward Hill, MA, USA, 99%+), chloroform-d (99.8 atom %d; Sigma-Aldrich), aluminum oxide (Carlo Erba, Val de Reuil, France, GPR). Solvents were HPLC or analytical grade. All chemicals were used as received.

2.2. Instrumentation

Reactions were carried out in round-bottomed flasks (50 mL, 100 mL), partially immersed in mineral oil heated on an IKA C-MAG HS 7 hotplate fitted with an IKA ETS-D5 temperature probe. Reactions were monitored by thin-layer chromatography (TLC) using alumina foil plates (200 μm thickness, <60 μm particle size; Sigma-Aldrich), spotted with homemade capillary tubes. The developed plates were viewed with a 365 nm UV lamp. Melting points were measured using a Stuart SMP40 melting point apparatus. NMR spectra were obtained with a Bruker Advance III HD NMR spectrometer equipped with an 11.75 Tesla magnet operating at 500.13 MHz and 125.76 MHz for ^{1}H and ^{13}C, respectively. Chemical shifts are reported downfield from tetramethylsilane (TMS) at 0.00 ppm. The data were processed using Topspin Software (Version 3.6.). Infra-red spectra were measured as KBr discs or on a NaCl plate using a Shimadzu IR-Affinity-1 spectrophotometer. The peak intensities are indicated as strong (s), medium (m), or weak (w). Mass spectrometry and exact mass measurements were performed by Medac Ltd. (Chobham, UK). UV–visible absorption and fluorescence emission spectra were obtained using a Jasco V-650 spectrophotometer and Jasco FP-8300 spectrofluorimeter at room temperature in $10 \times 10 \times 30$ mm Suprasil quartz cuvettes. A Hanna pH 210 Microprocessor pH meter, calibrated with buffer solutions at pH 7.0 and pH 4.0, was used to monitor the pH.

2.3. Synthesis
2.3.1. Method 1

2,6-Dibromonaphthalene-1,4,5,8-tetracarboxylic dianhydride (1.0 g, 2.3 mmol), *N,N*-dimethylethylenediamine (0.74 mL, 6.9 mmol) and 10 mL of glacial acetic acid were added to a 100 mL round-bottom flask, and the mixture refluxed at 130 °C for 30 min. The cooled solution was neutralized with saturated $NaHCO_3$ solution and extracted with chloroform (3×50 mL). Removal of the solvent by rotary evaporator yielded 1.13 g of intermediate **5** as a yellow powder.

Compound **5**

Yield = 85%; R_f = 0.31 (5:1 (*v/v*) CH_2Cl_2/MeOH); m. p. > 300 °C; ^{1}H NMR (CDCl$_3$, ppm): δ_H 8.98 (s, 2H), 4.34 (t, *J* = 6.7 Hz, 4H), 3.70 (s, 12H), 2.66 (t, *J* = 6.7 Hz, 4H); ^{13}C NMR (CDCl$_3$, ppm): δ_C 164.2, 164.1, 146.5, 134.4, 130.0, 126.8, 123.9, 122.2, 121.7, 120.9, 119.0, 118.1, 56.6, 52.2, 45.2, 44.7, 37.6, 32.0, 29.7, 25.8, 24.5, 22.7; IR (NaCl, cm^{-1}): 3064 (w), 2941 (w), 2868 (w), 1703 (m), 1659 (s), 1589 (m), 1435 (m), 1391 (m), 1377 (m), 1199 (m).

Then, excess pyrrolidine (12 mL, 0.14 mol) and intermediate **5** (0.20 g, 0.35 mol) were added to a round-bottom flask and warmed at 50 °C for 24 h. After the mixture cooled, the excess pyrrolidine was removed by rotary evaporator. The crude product was extracted with chloroform (5×20 mL) and washed with water. Removal of the solvent provided a crystalline black solid.

Compound **1**

Yield = 50%; R_f = 0.60 (5:1 (*v/v*) CH_2Cl_2/MeOH); black solid; m. p. > 300 °C; ^{1}H NMR (CDCl$_3$, ppm): δ_H 8.36 (s, 2H), 4.34 (t, *J* = 6.8 Hz, 4H), 3.49 (s, 8H), 2.63 (t, *J* = 6.8 Hz, 4H), 2.33 (s, 12H), 2.06 (s, 8H); ^{13}C NMR (CDCl$_3$, ppm): δ_C 163.76, 161.87, 147.39, 124.73, 122.42, 121.31, 105.37, 57.26, 52.56, 45.76, 38.49, 25.95; IR (NaCl, cm^{-1}): 2972 (m), 2868 (w), 2775 (w), 1681 (m), 1651 (s), 1585 (s), 1556 (s), 1496 (s), 1456 (m), 1393 (m), 1371 (m), 1190 (m), 1143 (m), 790 (m); HRMS (ESI-ToF): *m/z* cal. $C_{30}H_{39}N_6O_4$ [M+H] 547.3020, found 547.3033.

2.3.2. Method 2

2,6-Dibromonaphthalene-1,4,5,8-tetracarboxylic dianhydride was reacted at a 1:2 ratio in 4 mL of DMF for 1.5 h at 60 °C. Reaction completion was confirmed by TLC on alumina plates. To the same flask, 7 times excess of cyclic amine (pyrrolidine, morpholine, piperidine or azepane) was added and the solution was left overnight at 60 °C. Completion was confirmed by TLC. Then, 40 mL of heptane was added to the flask to form an azeotrope, and the solution was evaporated under vacuum by rotary evaporator. The residue was dissolved in 30 mL of chloroform, transferred to a separatory funnel and washed twice with water (2 × 30 mL). The chloroform layer was dried over sodium sulfate, gravity filtered and the solvent removed by rotary evaporator. The product was purified by column chromatography on alumina with dichloromethane as the initial eluent, and the polarity was gradually increased with methanol. The products were obtained as crystalline purple solids.

Compound **2**

Yield = 10%; R_f = 0.87 (6:4 (*v/v*) CH_2Cl_2/MeOH); m. p. = 200–202 °C; ^{1}H NMR (CDCl$_3$, ppm): δ_H 8.42 (s, 2H), 4.34 (t, *J* = 6.6 Hz, 4H), 3.99 (t, *J* = 4.6 Hz, 4H), 3.41 (t, *J* = 4.4 Hz, 4H), 2.67 (t, *J* = 6.2 Hz, 4H), 2.33 (s, 12H); ^{13}C NMR (CDCl$_3$, ppm): δ_C 162.94, 162.07, 151.91, 125.98, 124.80, 124.76, 110.47, 67.01, 57.27, 52.59, 45.76, 38.38; IR (KBr, cm^{-1}): 3007 (m), 2958 (m), 2862 (m), 2815 (m), 2763 (m), 1689 (s), 1649 (s), 1643 (s), 1571 (s), 1446 (s), 1313 (m), 1251 (m), 1228 (s), 1195 (s), 1166 (m), 1112 (m), 1062 (m), 1008 (w), 964 (w), 925 (w), 894 (w), 790 (w), 767 (m); HRMS (ESI ToF): *m/z* cal. $C_{30}H_{39}N_6O_6$ [M+H] 579.2931, found 579.2952.

Compound **3**

Yield = 20%; R_f = 0.82 (6:4 (*v/v*) CH_2Cl_2/MeOH); m. p. = 195–197 °C; ^{1}H NMR (CDCl$_3$, ppm): δ_H 8.42 (s, 2H), 4.33 (t, *J* = 6.9 Hz, 4H), 3.38 (m, 4H), 2.62 (t, *J* = 6.9 Hz, 4H), 2.33 (s, 12H), 1.83 (m, 4H), 1.77 (m, 2H); ^{13}C NMR (CDCl$_3$, ppm): δ_C 163.32, 162.11, 152.12, 125.50, 125.41, 124.32, 109.32, 57.40, 53.62, 45.88, 38.56, 26.27, 24.16; IR (KBr, cm^{-1}): 3022 (m), 2937 (m), 2858 (m), 2814 (m), 2762 (m), 1689 (s), 1654 (s), 1647 (s), 1568 (m), 1446 (m), 1359 (m), 1315 (m), 1265 (m), 1215 (m), 1188 (m), 1153 (m), 1114 (m), 1060 (w), 1006 (w), 790 (w), 759 (m); HRMS (ESI ToF): *m/z* cal. $C_{32}H_{43}N_6O_4$ [M+H] 575.3346, found 575.3355.

Compound **4**

Yield = 15%; R_f = 0.85 (6:4 (*v/v*) CH_2Cl_2/MeOH); m. p. = 154–156 °C; ^{1}H NMR (CDCl$_3$, ppm): δ_H 8.46 (s, 2H), 4.33 (t, *J* = 6.8 Hz, 4H), 3.56 (t, *J* = 5.3 Hz, 4H), 2.63 (t, *J* = 6.8 Hz, 4H), 2.33 (s, 12H), 1.90 (s, 4H), 1.61 (s, 4H); ^{13}C NMR (CDCl$_3$, ppm): δ_C 163.76, 162.95, 150.44, 125.57, 123.19, 122.99, 106.20, 57.42, 53.66, 45.87, 38.53, 28.42, 28.38; IR (KBr, cm^{-1}): 3005 (m), 2929 (m), 2848 (m), 2814 (m), 2763 (m), 1683 (s), 1643 (s), 1637 (s), 1564 (s), 1489 (m), 1361 (m), 1319 (m), 1273 (s), 1230 (s), 1192 (m) (s), 1165 (m), 1097 (w), 1043 (w), 1016 (w), 786 (m), 761 (m); HRMS (ESI ToF): *m/z* cal. $C_{34}H_{47}N_6O_4$ [M+H] 603.3659, found 603.3683.

2.4. Fluorescence Quantum Yields

Fluorescent quantum yields (Φ_f) were measured in 1:1 (*v/v*) methanol/water using the absorbance and fluorescence emission spectra according to Equation (1) [35]. Anthracene in ethanol was used as the standard (Φ_f = 0.27), excited at 375 nm, and fluorescein in 0.1 M water (Φ_f = 0.95) was excited at 450 nm. The equation relates the fluorescence quantum yield of the sample (Φ_f) to the fluorescence quantum yield of the standard (Φ_{ref}), the absorbance at λ_{max} (*Abs*), the area under the fluorescence emission curve (*A*), the refractive index of the solvent (η) and the refractive index of ethanol (η_{ref}).

$$\Phi_f = \Phi_{Ref}\left(\frac{Abs}{Abs_{ref}}\right)\left(\frac{A_{ref}}{A}\right)\left(\frac{\eta^2}{\eta_{ref}^2}\right) \tag{1}$$

2.5. Spectroscopic Measurements

Solutions of **1**–**4** were prepared from 1–5 mg of sample in 1:1 (*v*/*v*) methanol/water in 100 mL volumetric flasks and diluted to an absorbance less than 0.1 for the fluorescence measurements. The solution was monitored with a pH meter between pH 2 and pH 10 and stirred between each pH adjustment. The pH was adjusted using aqueous HCl and KOH solutions. The acid dissociation constants ($p\beta_{H+}$) were determined from absorbance and fluorescence intensity–pH plots fitted to the Henderson–Hasselbalch equation adapted for spectroscopic measurements in Equation (2) [36] and Equation (3) [37].

$$\log\left(\frac{A_{F_{max}} - A}{A - A_{F_{min}}}\right) = pH - p\beta_{H^+} \tag{2}$$

$$\log\left(\frac{I_{F_{max}} - I}{I - I_{F_{min}}}\right) = pH - p\beta_{H^+} \tag{3}$$

3. Results and Discussion

The pH indicators **1**–**4** were synthesized as illustrated in Figure 1. 2,6-Dibromonaphthalene-1,4,5,8-tetracarboxylic dianhydride was reacted with two equivalents of *N,N*-dimethylethylenediamine in *N,N*-dimethylformamide (DMF). The cyclic amine (piperidine, morpholine, piperidine or azepane) was subsequently added to the flask in excess (1:7 ratio) and the mixture was heated overnight. Following a work-up, the purple solids were purified by column chromatography on alumina with dichloromethane and methanol. The products were obtained as dark purple crystalline powders in 10–50% yield. They were characterized by ^{1}H and ^{13}C NMR, FTIR and HRMS. Characterization data are provided in the Materials and Methods section and the corresponding spectra are available in the Electronic Supplementary Information (Figures S1–S16).

The ^{1}H and ^{13}C NMR spectra were recorded in deuterated chloroform (Figures S1–S8, Supplementary Materials). Due to the symmetry within the molecules, only one aromatic ^{1}H peak is observed at 8.42 ppm. The triplets at 2.63 ppm and 4.34 ppm are assigned to the ethylene protons within the *N,N*-dimethylethylenediamine fragment and the singlet at 2.33 ppm is assigned to the four methyl groups. The most distinguishing resonances are those associated with the heterocyclic side groups. The morpholine moiety is observed at 3.42 ppm and 4.00 pm, the piperidine at 1.77, 1.83 and 3.38 ppm, and the azepane at 1.61, 1.90 and 3.56 ppm.

The UV–vis absorbance analysis was performed in 1:1 (*v*/*v*) methanol/water by potentiometric titration as a function of pH between pH 2 and pH 10 (Figure 2 and Figure S18). Isosbestic points were observed for **1** at 393 nm, 435 nm and 503 nm around pH 2, accompanied by a colour change from blue to purple to pink (Figure 3a). For **3** and **4**, the addition of HCl resulted in isosbestic points at 383 nm and 578 nm, and 377 nm and 563 nm, respectively. Compounds **2**–**4** are blue coloured solutions at neutral pH (Figure 3b). Upon addition of 1 M HCl, solutions of **3** and **4** readily turned violet. A colour change was not readily observed for **2** at pH 2, the solution remaining blue. However, the addition of a drop of concentrated HCl conjured a pink solution. A summary of UV–vis spectroscopic data is given in Table 2.

Compound **1** was qualitatively tested in chloroform, tetrahydrofuran and methanol. The λ_{abs} are similar at 611 nm, 609 nm and 600 nm. The molar extinction coefficient, expressed as log ε, are 3.87, 4.18 and 4.00.

Emission spectra were obtained by exciting at the isosbestic ca. 375 nm (Figure 4). All the compounds exhibited an increase upon addition of H$^+$ ion, with λ_{max} at ca. 450 nm. A significant increase in the fluorescence intensity was observed between pH 2.0 and 4.0 according to an off–on H$^+$-driven YES logic gate. This observation suggests that at low pH, a carbonyl oxygen of the NDI is protonated, leading to an increase in the intensity value. Fluorescence *turn-on* enhancements are promising at 10–37 fold (Table 2). However, the emission of **1**–**4** is very weak even in the presence of acid. The Φ_f in all cases is less (< 0.004),

such that the fluorescence is not detectable with the naked eye. From the viewpoint of a human observer, these chemosensors function as fluorimetric PASS 0 logic gates. The Φ_f of the core unsubstituted *N,N*-dimethylethyleneamine NDI is only 0.002. The addition of the heterocyclic substituents has a negligible effect on enhancing the fluorescence quantum yield. Excitation at 500 nm reveals another set of emission bands at 562 nm, 556 nm, 564 nm and 601 nm for **1–4** (Figure S18). Despite promising off–on switching ratios of 13, 10, 4 and 11, respectively, the maximum Φ_f at pH 2 is $\Phi_f \leq 0.0012$.
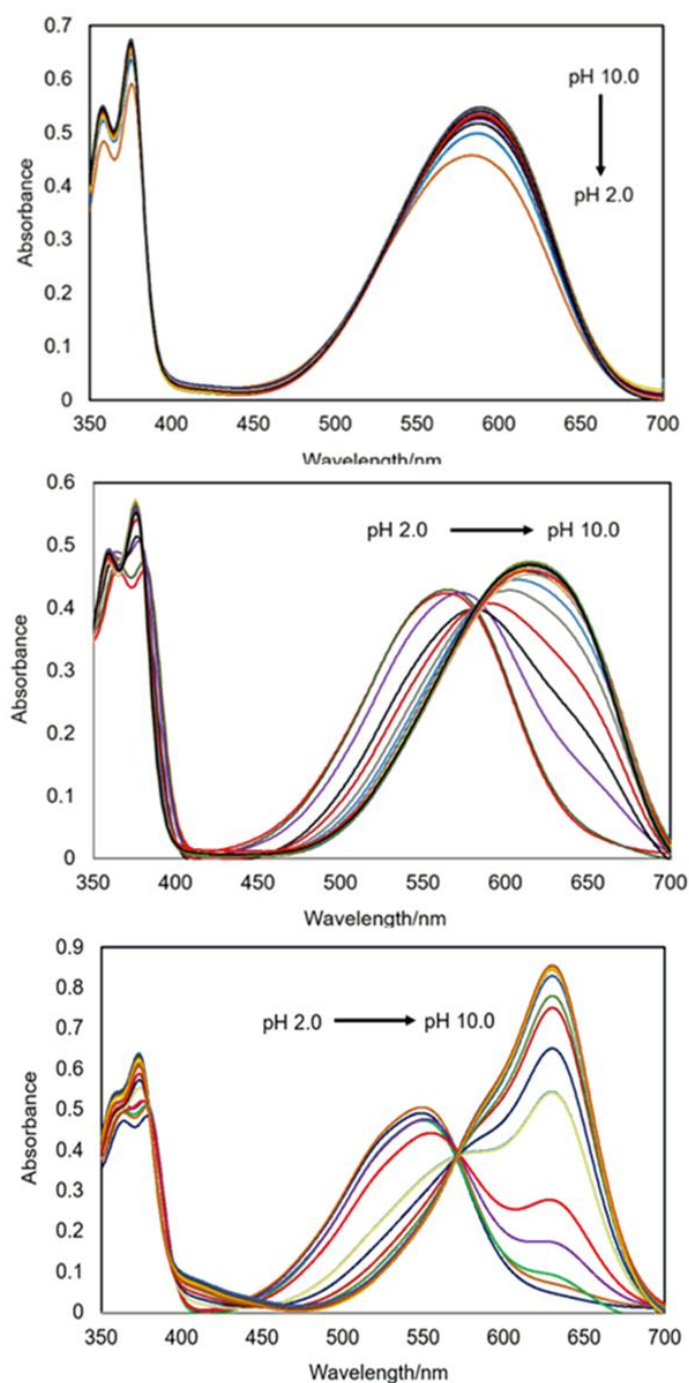

Figure 2. UV–visible absorbance spectra of 57 μM **2** (**top**), 89 μM **3** (**middle**) and 32 μM **4** (**bottom**) in 1:1 (*v/v*) methanol/water between pH 2 and pH 10. The spectra of **1** are available in the ESI (Figure S17).
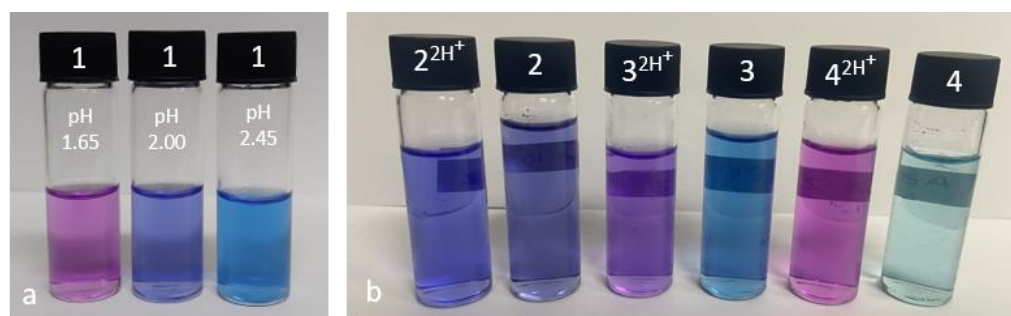
Figure 3. (a) Solutions of 10^{-5} M **1** (pyrrolidine) at pH 1.65 (pink), 2.00 (purple) and 2.45 (blue). (b) Solutions of 10^{-5} M **2–4** with **2** (morpholine), **3** (piperidine) and **4** (azepane) at $10^{-2.5}$ M H$^+$ (left, labelled 2H$^+$) and 10^{-10} M H$^+$ (right) in 1:1 (*v/v*) methanol/water.

Table 2. Physicochemical parameters of 10^{-5} M **1–4** measured by UV–visible absorption and fluorescence spectroscopy in 1:1 (*v/v*) methanol/water.

Parameter.	1	2	3	4
$\lambda_{max\,(pH\,3)}/nm$	368, 547, 617	358, 374, 595	360, 383, 565	362, 378, 550
Log ε (cm^{-1} mol^{-1} L) [a]	3.94	4.31	4.29	4.40
$\lambda_{max\,(pH\,10)}/nm$	366, 616	356, 377, 595	360, 376, 612	362, 373, 628
Log ε (cm^{-1} mol^{-1} L) [a]	4.00	4.26	4.50	4.34
λ_{isos}/nm	393, 435, 563	—[b]	383, 578	377, 563
pK_a	2.15	<2.0 [c]	2.91	3.38
$\lambda_{fluex375\,(pH\,3)}/nm$	451	450	450	452
$\Lambda_{fluex375\,(pH\,10)}/nm$	423	425	422	474
$\Phi_{f\,(>pH\,3)}$[d]	0.0010	0.0016	0.0037	0.0021
$\Phi_{f\,(pH\,10)}$[d]	0.0001	0.0001	0.0001	0.0001
$\lambda_{fluex500\,(pH\,2)}/nm$ [e]	562	556	564	601
Log P (2H$^+$) [f]	1.92	−0.07	2.83	3.75
Log P [f]	2.14	0.71	2.97	3.81

[a] Reported log ε for the longest wavelength. [b] No isosbestic point observed between pH 3.0 and pH 10.0. [c] A pK_a was not determined by UV–visible absorbance spectroscopy. [d] Fluorescent quantum yields relative to anthracene in ethanol (Φ_f = 0.27). [e] Emission spectra (Figure S18) are available in the ESI. $\Phi_f \leq 0.0012$ versus fluorescein in 0.1 M water (Φ_f = 0.95). [f] Log P values obtained from Chemdraw version 12.0.2.1076.

A recent study by Mukhopadhyay provides some insight into how we may overcome these limitations [38]. The introduction of amine (NH$_2$) or secondary amine (NHR) groups on the aromatic core results in enhanced quantum yields in aprotic solvents, such as DMSO (Φ_f = 0.679). The rationale for this large fluorescence enhancement is an excited state intramolecular proton transfer (ESIPT) via a six-membered transition state with a carbonyl. The substitution of one NH$_2$ with piperidine destabilizes the excited state, resulting in a Φ_f of 0.041. Within the same study, it was also demonstrated that the fluorescence of the disubstituted NH$_2$−NDI was sensitive to water, and was observed to decrease by 140-fold, resulting in the turning off of the fluorescence. Intermolecular hydrogen bonding between NHR groups, and perhaps the carbonyls too, with water molecules is suggested to prevail over the intramolecular N−H···O interactions with the imide carbonyl, which leads to deactivation of the ESIPT process and a low fluorescence output.

The NDIs have a hydrophobic naphthyl core and four polar carbonyl groups. The incorporation of the azacyclic hydrocarbon decreases the water solubility properties of NDI indicators. cLog P of the dimethylethyleneamine unsubstituted NDI is 0.59 when double protonated and 0.94 in the neutral state. The heterocyclic rings at the bay positions increase the lipophilicity by an order of magnitude for each methylene unit increase in the ring size to 1.92, 2.83 and 3.75 in the doubly protonated states for 1, 3 and 4, respectively. In the neutral states, the cLog **P values** are slightly higher at 2.14, 2.83 and 3.81. In contrast, **2** with the morpholino moiety, which includes an oxygen atom within the cyclic structure, has

a cLog P of -0.07 for the doubly protonated species and 0.71 for the neutral molecule. We observe that a remedy for increasing the solubility of ring-substituted NDI is to introduce an oxygen atom within the heterocyclic substituent, which allows for hydrogen bonding with the protic solvent. This strategy is commonly exploited in drug development [39].
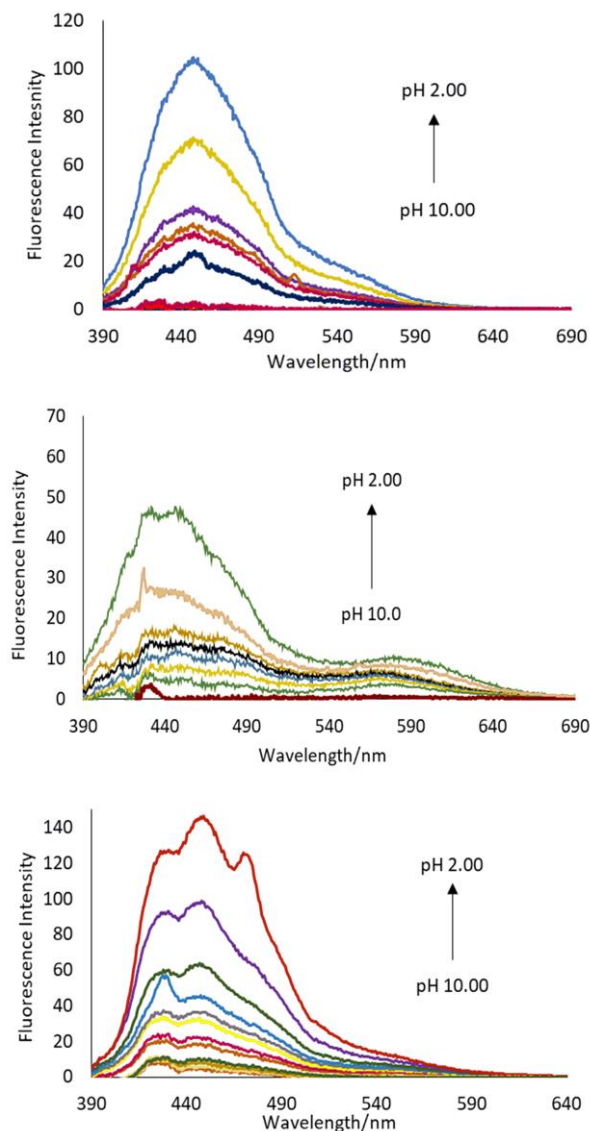
Figure 4. The emission spectra excited at 375 nm of **2** (**top**), **3** (**middle**) and **4** (**bottom**), with increasing acidity between pH 2–10.

4. Conclusions

Four naphthalenediimide pH indicators with *N,N*-dimethylethyleneamine at the imide positions and 5- to 7-membered heterocyclic rings at the bay positions were synthesized and studied in 1:1 (*v*/*v*) methanol/water. All of the compounds underwent distinct colour changes in the presence of acid, from blue under basic and neutral conditions to purple at acidic conditions. The compounds are weakly fluorescent in aqueous methanol, with fluorescence quantum yields below naked eye detection. A remedy for future work will be to replace the cyclic tertiary amines at the bay positions with secondary amines [33], which opens up the possibility of dual-mode colorimetric and fluorescent NDI indicators [40] and the development of Pourbaix sensors for environment protection, corrosion detection [29] and cellular imaging [41], among various other applications [26].

Supplementary Materials: The following supporting information can be downloaded at: https: //www.mdpi.com/article/10.3390/chemosensors11070360/s1, purifications, techniques, instrumentation and Figures S1–S16 (^{1}H NMR, ^{13}C NMR, FTIR and HRMS), Figure S17 (UV spectra of **1**) and Figure S18 (emission spectra of **1–4**).

Author Contributions: Conceptualization, D.C.M.; synthesis, F.M. and L.C.; formal analysis, F.M. and L.C.; investigation, F.M. and L.C.; writing—original draft, review and editing, D.C.M.; supervision, D.C.M. All authors have read and agreed to the published version of the manuscript.

Funding: The research was supported by the University of Malta.

Data Availability Statement: Data is available on request.

Conflicts of Interest: The authors declare no conflict of interest.

References

1. Pantos, G.D. *Naphthalenediimide and Its Congeners: From Molecules to Materials*; CPI Group: Croydon, UK, 2017.
2. Bhosale, S.V.; Al Kobaisi, M.; Jadhav, R.W.; Morajkar, P.P.; Jones, L.A.; George, S. Naphthalene diimides: Perspectives and promise. *Chem. Soc. Rev.* **2021**, *50*, 9845–9998. [CrossRef]
3. Al Kobaisi, M.; Bhosale, S.V.; Latham, K.; Raynor, A.M.; Bhosale, S.V. Functional Naphthalene Diimides: Synthesis, Properties, and Applications. *Chem. Rev.* **2016**, *116*, 11685–11796. [CrossRef]
4. Bhosale, S.V.; Jani, C.H.; Langford, S.J. Chemistry of naphthalene diimides. *Chem. Soc. Rev.* **2008**, *37*, 331–342. [CrossRef] [PubMed]
5. Sakai, N.; Mareda, J.; Vauthey, E.; Matile, S. Core-substituted naphthalenediimides. *Chem. Commun.* **2010**, *46*, 4225–4237. [CrossRef] [PubMed]
6. Supur, M.; El-Khouly, M.E.; Seok, J.H.; Kay, K.-Y.; Fukuzumi, S. Elongation of Lifetime of the Charge-Separated State of Ferrocene-Naphthalenediimide-[60]Fullerene Triad via Stepwise Electron Transfer. *J. Phys. Chem. A* **2011**, *115*, 14430–14437. [CrossRef]
7. Jameel, M.A.; Chien-Jen Yang, T.; Wilson, G.J.; Evans, R.A.; Gupta, A.; Langford, S.J. Naphthalene diimide-based electron transport materials for perovskite solar cells. *J. Mater. Chem. A* **2021**, *9*, 27170–27192. [CrossRef]
8. Shukla, J.; Mukhopadhyay, P. Synthesis of Functionalized Naphthalene Diimides and their Redox Properties. *Eur. J. Org. Chem.* **2019**, 7770–7786. [CrossRef]
9. Thalacker, C.; Röger, C.; Würthner, F. Synthesis and Optical and Redox Properties of Core-Substituted Naphthalene Diimide Dyes. *J. Org. Chem.* **2006**, *71*, 8098–8105. [CrossRef]
10. Cox, R.P.; Higginbotham, H.F.; Graystone, B.A.; Sandanayake, S.; Langford, S.J.; Bell, T.D.M. A new fluorescent H^{+} sensor based on core-substituted naphthalene diimide. *Chem. Phys. Lett.* **2012**, *521*, 59–63. [CrossRef]
11. Doria, F.; Gallati, C.M.; Freccero, M. Hydrosoluble and solvatochromic naphthalene diimides with NIR absorption. *Org. Biomol. Chem.* **2013**, *11*, 7838–7842. [CrossRef] [PubMed]
12. Weißenstein, A.; Grande, V.; Saha-Möller, C.R.; Würthner, F. Water-soluble naphthalene diimides: Synthesis, optical properties, and colorimetric detection of biogenic amines. *Org. Chem. Front.* **2018**, *5*, 2641–2651. [CrossRef]
13. Ghule, N.V.; Bhosale, R.S.; Kharat, K.; Puyad, A.L.; Bhosale, S.V.; Bhosale, S.V. A Naphthalenediimide-Based Fluorescent Sensor for Detecting the pH within the Rough Endoplasmic Reticulum of Living Cells. *ChemPlusChem* **2015**, *80*, 485–489. [CrossRef] [PubMed]
14. Doria, F.; Folini, M.; Grande, V.; Cimino-Reale, G.; Zaffaroni, N.; Freccero, M. Naphthalene diimides as red fluorescent pH sensors for functional cell imaging. *Org. Biomol. Chem.* **2015**, *13*, 570–576. [CrossRef]
15. Doria, F.; Nadai, M.; Sattin, G.; Pasotti, L.; Richter, S.N.; Freccero, M. Water soluble extended naphthalene diimides as pH fluorescent sensors and G-quadruplex ligands. *Org. Biomol. Chem.* **2012**, *10*, 3830–3840. [CrossRef] [PubMed]
16. Lu, X.; Zhu, W.; Xie, Y.; Li, X.; Gao, Y.; Li, F.; Tian, H. Near-IR Core-Substituted Naphthalenediimide Fluorescent Chemosensors for Zinc Ions: Ligand Effects on PET and ICT Channels. *Chem. Eur. J.* **2010**, *16*, 8355–8364. [CrossRef]
17. Hughes, W.; Rananaware, A.; La, D.D.; Jones, L.A.; Bhargava, S.; Bhosale, S.V. Aza-crown ether-core substituted naphthalene diimide fluorescence "turn-on" probe for selective detection of Ca^{2+}. *Sens. Actuators B Chem.* **2017**, *244*, 854–860. [CrossRef]
18. Cox, R.P.; Sandanayake, S.; Scarborough, D.L.A.; Izgorodina, E.I.; Langford, S.J.; Bell, T.D.M. Investigation of cation binding and sensing by new crown ether core substituted naphthalene diimide systems. *New J. Chem.* **2019**, *43*, 2011–2018. [CrossRef]
19. Hangarge, R.V.; La, D.D.; Boguslavsky, M.; Jones, L.A.; Kim, Y.S.; Bhosale, S.V. An Aza-12-crown-4 Ether-Substituted Naphthalene Diimide Chemosensor for the Detection of Lithium Ion. *ChemistrySelect* **2017**, *2*, 11487–11491. [CrossRef]
20. Bora, H.J.; Barman, P.; Bordoloi, S.; Gogoi, G.; Gogoi, B.; Sarma, N.S.; Kalita, A. Realization of multi-configurable logic gate behaviour on fluorescence switching signalling of naphthalene diimide congeners. *RSC Adv.* **2021**, *11*, 35274–35279. [CrossRef]
21. Ajayakumar, M.R.; Hundal, G.; Mukhopadhyay, P.A. Tetrastable naphthalenediimide: Anion induced charge transfer, single and double electron transfer for combinational logic gates. *Chem. Commun.* **2013**, *49*, 7684–7686. [CrossRef]
22. Jiang, W.; Han, M.; Zhang, H.-Y.; Zhang, Z.-J.; Liu, Y. A Double Plug–Socket System Capable of Molecular Keypad Locks through Controllable Photooxidation. *Chem. Eur. J.* **2009**, *15*, 9938–9945. [CrossRef]

23. Magri, D.C. Recent Progress on the Evolution of Pourbaix Sensors: Molecular Logic Gates for Protons and Oxidants. *Chemosensors* **2018**, *6*, 48. [CrossRef]

24. Magri, D.C. Logical sensing with fluorescent molecular logic gates based on photoinduced electron transfer. *Coord. Chem. Rev.* **2021**, *426*, 213598. [CrossRef]

25. Vella Refalo, M.; Farrugia, N.V.; Johnson, A.D.; Klejna, S.; Szaciłowski, K.; Magri, D.C. Fluorimetric naphthalimide-based polymer logic beads responsive to acidity and oxidisability. *J. Mater. Chem. C* **2019**, *7*, 15225–15232. [CrossRef]

26. Magri, D.C. 'Pourbaix sensors': Fluorescent molecular logic gates for pE and pH. *Supramol. Chem.* **2017**, *29*, 741–748. [CrossRef]

27. Farrugia, T.J.; Magri, D.C. 'Pourbaix sensors': A new class of fluorescent pE–pH molecular AND logic gates based on photoinduced electron transfer. *New J. Chem.* **2013**, *37*, 148–151. [CrossRef]

28. Grech, J.; Spiteri, J.C.; Scerri, G.J.; Magri, D.C. Molecular logic with ferrocene-rylene conjugates: A comparison of naphthalenediimide, naphthalimide and perylenediimide Pourbaix sensor designs. *Inorg. Chim. Acta* **2023**, *544*, 121176. [CrossRef]

29. Scerri, G.J.; Spiteri, J.C.; Magri, D.C. Pourbaix sensors in polyurethane molecular logic-based coatings for early detection of corrosion. *Mater. Adv.* **2021**, *2*, 434–439. [CrossRef]

30. Cardona, M.A.; Magri, D.C. Synthesis and spectrophotometric studies of water-soluble amino[bis(ethanesulfonate)] azobenzene pH indicators. *Tetrahedron Lett.* **2014**, *55*, 4559–4563. [CrossRef]

31. Cardona, M.A.; Makuc, D.; Szaciłowski, K.; Plavec, J.; Magri, D.C. Water-Soluble Colorimetric Amino[bis(ethanesulfonate)] Azobenzene pH Indicators: A UV−Vis Absorption, DFT, and 1H−15NNMR Spectroscopy Study. *ACS Omega* **2017**, *2*, 6159–6166. [CrossRef] [PubMed]

32. Cardona, M.A.; Mallia, C.J.; Baisch, U.; Magri, D.C. Water-soluble amino(ethanesulfonate) and [bis(ethanesulfonate)] anthracenes as fluorescent photoinduced electron transfer (PET) pH indicators and Fe^{3+} chemosensors. *RSC Adv.* **2016**, *6*, 3783–3791. [CrossRef]

33. Bell, T.D.M.; Yap, S.; Jani, C.H.; Bhosale, S.V.; Hofkens, J.; De Schryver, F.C.; Langford, S.J.; Ghiggino, K.P. Synthesis and Photophysics of Core-Substituted Naphthalene Diimides: Fluorophores for Single Molecule Applications. *Chem. Asian J.* **2009**, *4*, 1542–1550. [CrossRef] [PubMed]

34. Maniam, S.; Higginbotham, H.F.; Bell, T.D.M.; Langford, S.J. Harnessing Brightness in Naphthalene Diimides. *Chem. Eur. J.* **2019**, *25*, 7044–7057. [CrossRef] [PubMed]

35. Valeur, B.; Berberan-Santos, M.N. *Molecular Fluorescence: Principles and Applications*; John Wiley & Sons: Weinheim, Germany, 2012.

36. de Silva, A.P.; Gunaratne, H.Q.N.; Lynch, P.L.M.; Patty, A.J.; Spence, G.L. Luminescence and Charge Transfer. Part 3. The Use of Chromophores with ICT (Internal Charge Transfer) Excited States in the Construction of Fluorescent PET (Photoinduced Electron Transfer) pH Sensors and Related Absorption pH Sensors with Aminoalkyl Side Chains. *J. Chem. Soc. Perkins Trans. 2* **1993**, 1611–1616. [CrossRef]

37. Bissell, R.A.; Calle, E.; de Silva, A.P.; de Silva, S.A.; Gunaratne, H.Q.N.; Habib-Jiwan, J.-L.; Annesley Peiris, S.L.; Rupasinghe, R.A.D.D.; Samarasinghe, T.K.S.D.; Sandanayake, K.R.A.S.; et al. Luminescence and Charge Transfer. Part 2. Aminomethyl Anthracene Derivatives as Fluorescent PET (Photoinduced Electron Transfer) Sensors for Protons. *J. Chem. Soc. Perkins Trans. 2* **1991**, 1559–1564. [CrossRef]

38. Keshri, S.K.; Mandal, K.; Kumar, Y.; Yadav, D.; Mukhopadhyay, P. Naphthalenediimides with High Fluorescence Quantum Yield: Bright-Red, Stable, and Responsive Fluorescent Dyes. *Chem. Eur. J.* **2021**, *27*, 6954–6962. [CrossRef]

39. Patrick, G.L. *An Introduction to Medicinal Chemistry*, 5th ed.; Oxford Press: Oxford, UK, 2013.

40. Zong, L.; Wang, C.; Song, Y.; Xie, Y.; Zhnag, P.; Peng, Q.; Li, Q. A dual-function probe based on naphthalene diimide for fluorescent recognition of Hg^{2+} and colorimetric detection of Cu^{2+}. *Sens. Actuators B Chem.* **2017**, *252*, 1105–1111. [CrossRef]

41. Johnson, A.D.; Buhagiar, J.A.; Magri, D.C. 4-Amino-1,8-naphthalimide–ferrocene conjugates as potential multi-targeted anticancer and fluorescent cellular imaging agents. *RSC Med. Chem.* **2021**, *12*, 2060–2064. [CrossRef]